0026-895X/91/040629-14$03.00/0

MOLECULAR PHARMACOLOGY, 39:629-642

Application of Pattern Recognition Methods to the Analysis and Classification of Toxicological Data Derived from Proton Nuclear Magnetic Resonance Spectroscopy of Urine

K. P. R. GARTLAND, C. R. BEDDELL, J. C. LINDON, and J. K. NICHOLSON

Department of Chemistry, Birkbeck College, University of London, London WC1H 0PP, UK (K.P.R.G., J.K.N.), and Department of Physical Sciences, The Wellcome Research Laboratories, Beckenham, Kent BR3 3BS, UK (C.R.B., J.C.L.)

Received September 6, 1990; Accepted January 18, 1991

SUMMARY

A computer-based pattern recognition (PR) approach has been applied to the classification and interrogation of ^{1}H NMR-generated urinalysis data, in a variety of experimental toxicity states in the rat. ^{1}H NMR signal intensities for each endogenous urinary metabolite were regarded as coordinates in multidimensional space and analyzed using PR methods, through which the dimensionality was reduced for display and categorization purposes. The changes in the NMR spectral patterns were characterized by 17 metabolic dimensions, which were then analyzed by employing the unsupervised learning methods of hierarchical cluster analysis, two-dimensional nonlinear map (NLM) analysis, and two- or three-dimensional principal components analysis (PCA). Different types of toxin (hepatotoxins and cortical and papillary nephrotoxins) were classified according to NMR-detectable biochemical effects. PCA provided consistently better results than NLMs in terms of discrimination of toxicity type, and maps based on correlation matrices also gave improved discrimination over those based on raw data. Various refinements in the data analysis were investigated, including taking NMR urinalysis data at three time points after exposure of the rats to six different nephrotoxins, as well as employing a dual-scoring system (time and magnitude of change). The maps generated from the time-course information produced the best discrimination between nephrotoxins from different classes. The robustness of the classification methods (in particular NLMs and PCA based on correlation matrices) and the influence of the addition of new scored biochemical data, reflecting dose-response situations, nutritional effects on toxicity, sex differences in biochemical response to toxins, the addition of a new toxin class (cadmium chloride, a testicular toxin and renal carbonic anhydrase inhibitor), and an additional metabolite descriptor (creatine), to the PR analysis were also evaluated. Initial training set maps were fundamentally stable to the addition of new data, and both NLM and PCA methods correctly "predicted" the toxicological effects from NMR data for test compounds, suggesting that the approach using PR and ^{1}H NMR urinalysis for the generation and classification of acute toxicological data has wide applicability.

High resolution proton NMR spectroscopic studies on body fluids and intact cell systems can provide detailed information on the biochemical and toxicological effects of a wide range of xenobiotic compounds (1–10). Although conventional enzymatic and chromatographic methods may be more sensitive than ^{1}H NMR in detecting low levels of metabolites in biological materials, significant analytical advantages may be gained by using ^{1}H NMR to follow biochemical responses to foreign compounds. In order to understand the potential role of NMR as a toxicological tool, it is first worth considering the conventional approach to solving a key question in mechanistic toxicology, i.e., What are the critical biochemical pathways affected by a toxin and how do they relate to the exhibited toxicological responses in the biological system? From an analytical viewpoint, this necessitates further questions. For example, what changes occur in cellular metabolite levels? Which metabolites should be measured and in what matrix? How do changes in the measured parameters in the chosen matrix (e.g., a body fluid or tissue sample) relate to the critical lesion? How can these data be used to classify and predict the type of toxicological lesion? Answering these important toxicological questions using conventional bioanalytical approaches usually requires the subjective selection of a battery of biochemical methods, often used in conjunction with histopathological techniques *in vivo* and in selected *in vitro* systems. This is necessarily a complex and time-consuming process, and if an inappropriate or restricted range of biochemical methods or metabolic parameters is chosen, important metabolic disturbances may be over-

ABBREVIATIONS: Hg, mercury II chloride; ALY, allyl alcohol; ANIT, α-naphthylisothiocyanate; BEA, 2-bromoethanamine hydrobromide; Cd, cadmium chloride; CrO_4, sodium chromate; DMA, dimethylamine; DMG, *N,N*-dimethylglycine; HCBD, hexachlorobutadiene; HCA, hierarchical cluster analysis; HYD, hydrazine; NLM, nonlinear map; PAP, *p*-aminophenol; PC, principal component; PCA, principal components analysis; PI, propylene imine; PR, pattern recognition; RCA, renal carbonic anhydrase; THIO, thioacetamide; TMAO, trimethylamine *N*-oxide; TSP, 3-trimethylsilyl-[2,2,3,3-$^2H_4$]1-propionate; UN, uranyl nitrate.

looked and the mode of toxicity poorly defined. ^{1}H NMR spectroscopy is well suited to the study of toxicological events, because multicomponent analyses on biological materials can be made simultaneously, without bias imposed by the experimenters' expectations of toxin-induced metabolic or biochemical changes. For example, the ^{1}H NMR spectrum of a biofluid or tissue extract gives a characteristic (fingerprint) pattern of resonances for a range of important endogenous metabolites that are represented in many key cellular biochemical processes (4, 9), notwithstanding the fact that end-stage changes in tissue (and hence biofluid) composition will also be superimposed on more specific biochemical effects of the toxins involved. Quantifiable changes in metabolite patterns may give information on the location and severity of a toxic lesion and also give insights into underlying molecular mechanisms of toxicity (1, 2, 5, 6). The application of ^{1}H NMR urinalysis to the study of the effects of region-specific nephrotoxins uncovered distinct abnormal patterns of metabolites that were apparently associated with different sites of nephrotoxic action (4). ^{1}H NMR data showed that proximal tubular toxins (Hg, PAP, and HCBD) caused reproducible time-course patterns of biochemical changes in the urine, comprising glycosuria, lactic aciduria, and aminoaciduria. Renal papillary toxins (PI and BEA) produced different abnormal excretion patterns in terms of both time course and composition of urinary metabolites (4). Chemically induced renal papillary necrosis produced early increases (within 8 hr) in urinary levels of DMA and TMAO, followed by later (24–48 hr) elevations in DMG, succinate, and acetate and decreases in TMAO and 2-oxoglutarate, and these are postulated as possible novel markers of experimental renal papillary damage (4). Hence, the ability of NMR methods to detect novel markers of toxicity (thus extending the number of available screening parameters) is a consequence of its exploratory analytical nature.

^{1}H NMR spectra of biofluids are extraordinarily rich in information on endogenous biochemical processes in health and disease (9) and, although absolute quantitation of metabolites can be readily achieved (1, 9), it is the overall pattern of the spectral data on metabolite relationships that appears to convey much of the information (4). The very complexity of the ^{1}H NMR spectra of biofluids from animals with biochemical lesions appears to necessitate the use of novel approaches to data analysis, if more detailed toxicological information is to be obtained from NMR spectra. In the present study, we have applied computer-based PR methodology to toxicological data derived from ^{1}H NMR analysis of urine obtained from rats exposed to the nephrotoxins Hg, PAP, HCBD, CrO_4, PI, and BEA and the hepatotoxins ANIT, CCl_4, HYD, and THIO and the testicular toxin Cd. Some of the basic work on the NMR-detectable changes in biochemical profiles has been published previously and analyzed using conventional statistical procedures (1–3, 6, 8). Data from these studies, together with new experimental toxicological information, have been used to form a "training set" with which to investigate the various PR approaches to the problem of classification of toxicity based only on ^{1}H NMR urinalysis results. Of the nephrotoxins, CrO_4 damages the pars convoluta of the proximal tubule (11); Hg, HCBD, and PAP all cause lesions in the pars recta of the proximal tubule (1, 5, 12, 13); and PI and BEA are inner medullary toxins that cause renal papillary necrosis (14, 15). Of the hepatotoxins, CCl_4 causes centrilobular necrosis with fatty liver (16); THIO causes centrilobular necrosis alone,

TABLE 1

Doses, routes, and vehicles employed for the administration of the toxic substances

All treatments were administered by intraperitoneal injection except CrO_4, which was administered by subcutaneous injection. M, male; F, female rats; SD, Sprague-Dawley; f, fed; *, fasted rats.

Treatment	Rat strain (*n*)	Dose	Vehicle	Urine collection points				
				0–8	8–24	24–48	0–6	6–24
				hr				
Training set: nephrotoxins								
PAP	F344 (3)	100 mg/kg	Saline	+	+	+	–	–
CrO_4	F344 (5)	20 mg/kg	Saline	+	+	+	–	–
Hg (f)	F344 (4)	2 mg/kg	Saline	+	+	+	–	–
HCBD	F344 (5)	200 mg/kg	Corn oil	+	+	+	–	–
PI	F344 (5)	20 μl/kg	Corn oil	+	+	+	–	–
BEA	F344 (5)	250 mg/kg	Corn oil	+	+	+	–	–
Test set I: nephrotoxins								
UN	F344 (3)	10 mg/kg	Saline	+	+	+	–	–
Hg*	SD (3)	0.5 mg/kg	Saline	+	+	–	–	–
Hg*	SD (3)	1.0 mg/kg	Saline	+	+	–	–	–
Hg*	SD (3)	1.5 mg/kg	Saline	+	+	–	–	–
Hg*	SD (3)	2.0 mg/kg	Saline	+	+	–	–	–
Training set: hepatotoxins								
THIO	Wistar (3)	200 mg/kg	Saline	–	–	–	+	+
HYD	Wistar (3)	60 mg/kg	Saline	–	–	–	+	+
CCl_4	Wistar (3)	2 ml/kg	Corn oil	–	–	–	+	+
ANIT	Wistar (3)	300 mg/kg	Arachis oil	–	–	–	+	+
Test set II: hepatotoxin								
Aly	Wistar (3)	50 μl/kg	Saline	–	–	–	+	+
Test set II: testicular toxins								
Cd (M)	SD (3)	6 μmol/kg	Saline	–	–	–	+	+
Cd (M)	SD (3)	9 μmol/kg	Saline	–	–	–	+	+
Cd (M)	SD (3)	12 μmol/kg	Saline	–	–	–	+	+
Cd (M)	SD (3)	24 μmol/kg	Saline	–	–	–	+	+
Cd (F)	SD (3)	24 μmol/kg	Saline	–	–	–	+	+

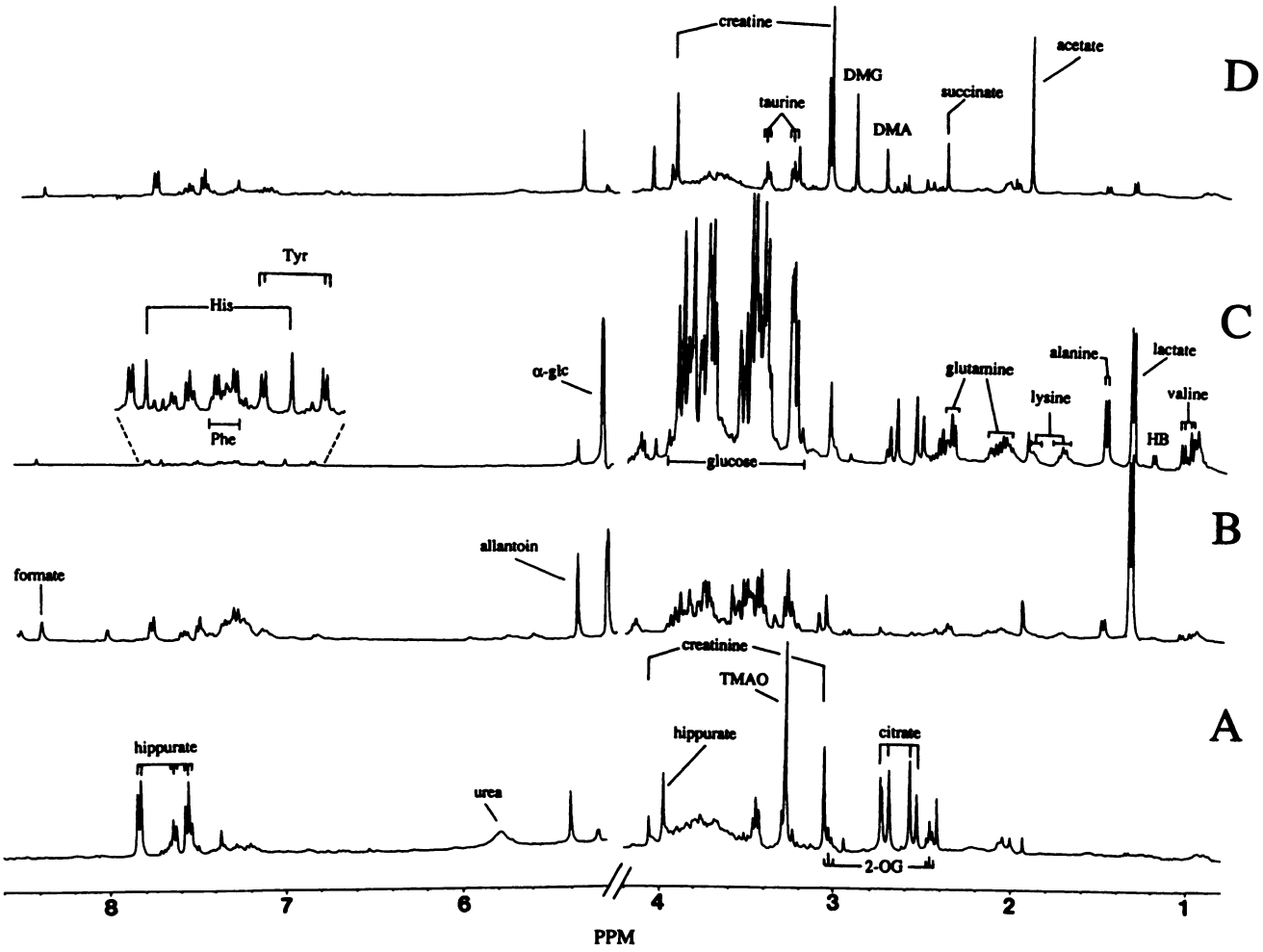

Fig. 1. ^{1}H NMR spectra (400 MHz) of urine obtained from a control rat (A) or from a rat 8–24 hr after dosing with 2 mg/kg Hg (B), 8–24 hr after 200 mg/kg HCBD (C) (both proximal tubular toxins), or 24–48 hr after 250 mg/kg BEA (a renal papillary toxin) (D). Times shown are when maximum biochemical effect was seen. See text for experimental conditions. *2-OG*, 2-oxoglutarate; *α-glc*, glucose.

whereas HYD causes fatty liver without necrosis (17, 18) and ANIT causes periportal liver necrosis with extrahepatic cholestasis and hyperbilirubinemia (19).

The main aim of this work was to evaluate the use of unsupervised learning PR methods in the classification of toxicity based on ^{1}H NMR data and to explore this approach to the prediction of toxic effects of model compounds based on biochemical inferences gained from ^{1}H NMR urinalysis studies. Subsequent to this, the effects of a number of biological variables, such as fasting, magnitude of dose, sex and strain of rat, and the addition of a new toxin class, were evaluated for their effects on the results obtained from the PR package. The "test set" toxins included Cd [a testicular toxin that also causes inhibition of RCA (8)], which was investigated in both male and female rats. A periportal hepatotoxin (ALY) and three proximal tubular toxins (UN, Hg under fasting conditions at various doses, and PAP at a lower dose than that used in the training set) were also included in the test set. The purpose of the test set data analysis was to evaluate the robustness of the PR methods, which were optimized by analysis of the training set data, and the predictive power of the unsupervised learning classification of the toxicity of the test set toxins, which was designed to simulate the addition of data on compounds with unknown toxicological dispositions.

Experimental Procedures

Animals and treatments. Wistar and Fischer 344 rats (all males except where stated) were housed individually in metabolism cages and allowed free access to food and tap water. Cages were placed in well ventilated animal rooms with regular light cycles (12-hr, 7:00 a.m. to 7:00 p.m.). Urine was collected over ice at various times after dosing with a range of selected hepatotoxins and nephrotoxins with different mechanisms and sites of action (see Table 1 for the number and strain of rats, treatments given, dose route, and vehicles used). Urinary volumes and pH values were recorded, and samples were then centrifuged at 3000 rpm for 10 min at 4°, to remove food particles and other debris. Toxins were supplied by Aldrich (ANIT, BEA, CCl_4, Cd, HCBD, PAP, CrO_4, and THIO), BDH (UN and Hg), and Sigma (ALY, HYD, and PI) and were used as received. NMR urinalysis data were obtained from rats receiving 10 mg/kg UN [a pars recta toxin (20, 21)], 50 mg/kg PAP, 50 μl/kg ALY [a periportal hepatotoxin (22)], or increasing doses (6–24 μmol/kg) of Cd [a testicular toxin and RCA inhibitor (8, 23)] and from fasted rats receiving increasing doses (0.5–2.0 mg/kg) of Hg (3). In this way, the six nephrotoxins and four hepatotoxins acted as the training set of metabolic data, whereas the data from the UN, PAP (50 mg/kg), ALY, fasted Hg, and Cd experiments acted as the test set. In the test set, the possible effects of various experimental conditions were examined, including fasting, sex differences, dose, and variation in rat strain. ^{1}H NMR urinalysis data from rats exposed to Cd, ALY, UN, and (fasted) Hg were obtained from our own previously published sources (1, 8, 18, 22).

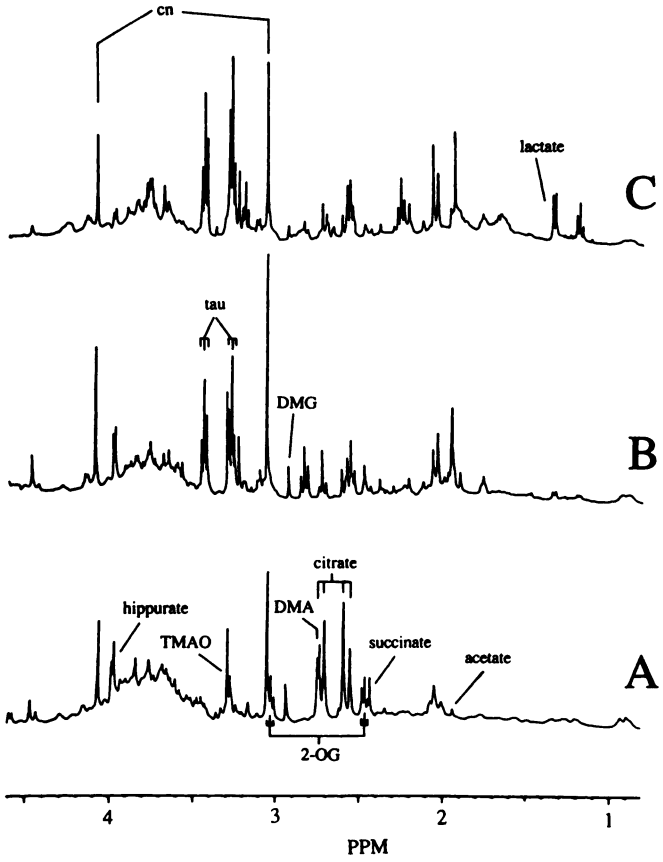

Fig. 2. ^{1}H NMR spectra (400 MHz) of urine from a Wistar rat −24–0 hr before (A) and 0–6 hr (B) and 6–24 hr (C) after dosing with 60 mg/kg HYD. See text for experimental conditions.

NMR urinalysis. NMR measurements were made at ambient probe temperature (298 ± 1K) with a Bruker WH400 spectrometer operating at 400.13 MHz proton resonance frequency and fitted with a 16-bit analog-to-digital converter, Aspect 3000 data system, and array processor. A calculated volume of urine (4) was lyophilized and redissolved in an equivalent volume of ^2H_2O containing sodium TSP (used as a secondary standard and assigned to $\delta = 0$ ppm), in 5-mm tubes. For each sample, ^{1}H NMR spectra were recorded using a spectral width of 5000 Hz, centered at the water resonance frequency. Sixty-four free induction decays were collected into 16,384 computer points (1.7-sec acquisition time), using 28° (3 μsec) pulses. An additional delay of 3.0 sec between pulses was added to ensure that the spectra were fully T_1 relaxed. A continuous secondary irradiation field at the resonance frequency of water was applied in order to suppress the residual water signal. This does not result in spectral distortion due to nuclear Overhauser effects or cross-relaxation in the system used. An exponential line-broadening function of 0.6 Hz was applied before Fourier transformation. Resonance assignments were confirmed by a combination of chemical shift, spin-spin coupling patterns, coupling constants, and, ultimately, standard additions (24).

Scoring of NMR-generated data: magnitude of change in metabolite levels. NMR spectra of urine specimens (containing equal concentrations of TSP) from rats exposed to six nephrotoxins and four hepatotoxins were compared with spectra obtained from untreated control animals at the same time point, plotted on the same vertical scale. Full spectral width spectra were plotted on a 120-cm horizontal expansion, and peak heights were measured. For partially overlapped signals, such as glutamine and valine (Fig. 1c), selected partial signals were measured. The following arbitrary seven-level scoring system was employed, relating to metabolite signal intensities and the added TSP standard and taking the modal score of each toxin for computer analysis:

+3 = a major elevation in urinary concentration, corresponding to times control level

+2 = an elevation in concentration corresponding to 2 to 3 times control level

+1 = a detectable but minor elevation in concentration, of up to 2 times control level

0 = not detectably different from control level

−1 = minor decrease (20–50%) from control levels

−2 = moderate decrease (50–90%) from control levels

−3 = signals from metabolite not detectable by NMR spectroscopy after toxin treatment, but metabolite is always detectable in controls measured under the same conditions

This procedure is rapid and easy to apply and generates a scaled matrix containing information on the changes in metabolite concentrations induced by various classes of toxin. Two scored data tables were produced that contain information on the maximal change at any time point produced by all the toxins [Table 2 was subdivided into training set (A) and test set (B) data] and information on the changes occurring at three time points after exposure to the nephrotoxins alone (Table 3). A third scoring table (Table 4) contains the nephrotoxin data, in which each metabolite has two scores, one for the time of maximum change and another for the magnitude of that change. The magnitude of change employed the same seven-level scoring system described above for each individual metabolite measured but with a second three-level descriptor to relate the magnitude of change to the time at which it occurred. Because there were three time points at which urine was sampled, these correspond to scores of 1, 2, and 3 for maximal changes at 8, 24, and 48 hr, respectively. Thus, for example, a score of +3,3 corresponds to a major elevation at 48 hr, whereas −2,1 would correspond to a moderate reduction at 8 hr. The score 0,0 would by definition indicate that control levels for that metabolite were maintained throughout the experiment. Table 4, therefore, gives the majority of the information in Table 3 but presented alternatively in a reduced form.

Computer data analysis. Data handling and analysis were performed using RS/1 (25) and the software package ARTHUR (26), running on a DEC VAX 8550 computer. The unsupervised learning PR methods used were NLM, PCA, and HCA. PR is a general term applied to methods of data analysis that can cope not only with fully quantitative data but also with discrete or scored data, for example, those obtained from histology or behavioral studies. The methods work in the multidimensional parameter space where, in this case, each dimension is the concentration of one metabolite or the time of effect, but they can also provide dimension-reduction techniques for display purposes.

HCA is a widely used method (27, 28) by which one measures the distances between all pairs of points, identifies the nearest pair, combines them into a new point midway between them (the centroid method), recalculates the distances from this new point to every other point in the data set, finds the new nearest pair, combines them, and so on, until all points have been linked. When a data (or combined) point is being combined with an already combined point, the new point is again obtained as an average, weighted by the respective number of data contributing to each point. The resulting structure can be displayed as a dendrogram, which shows at what degree of similarity each pair of points was combined (29). NLM techniques were introduced to the chemical literature by Kowalski and Bender (30), based on the method published by Sammon (31). These methods develop a correspondence where each point in the original data set is mapped onto a point in a two-dimensional plane. The interpoint distances in the two-dimensional plane are intended to mimic the interpoint distances in the original space, but such mapping inevitably involves error. Operationally, NLM is done by iteratively minimizing an error function by

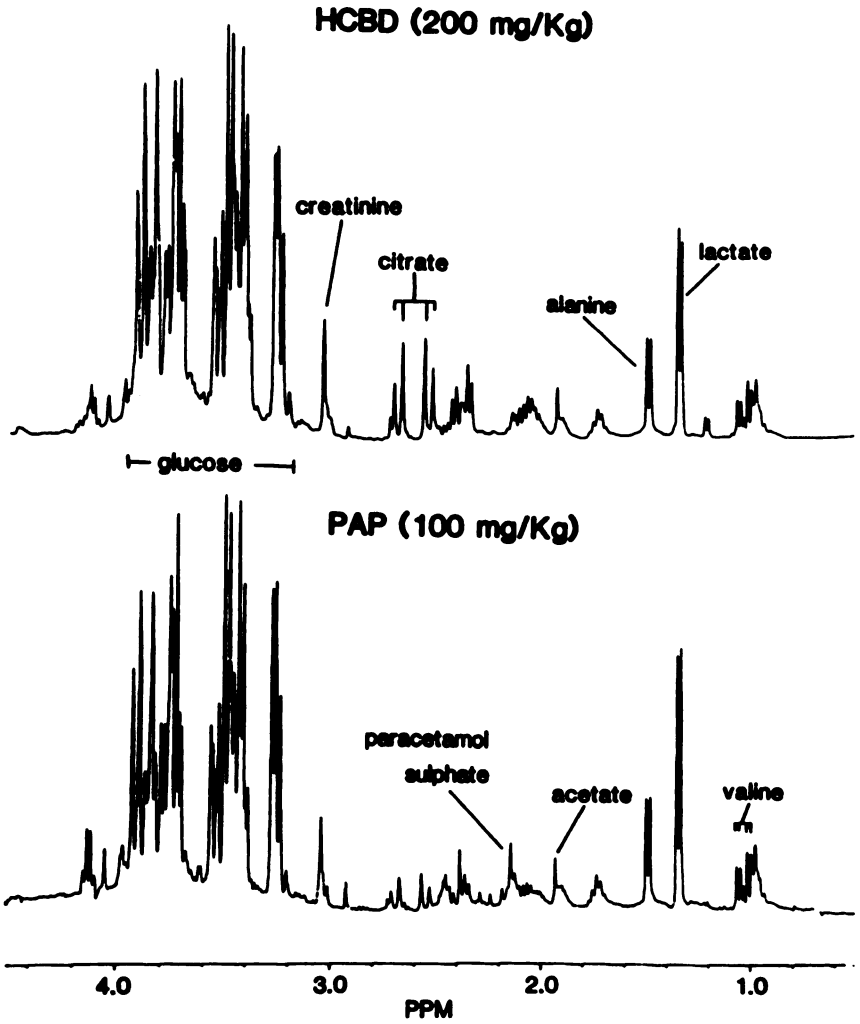

Fig. 3. Comparison of the ^{1}H NMR spectra of 16-hr (8–24 hr) urine from rats treated with 100 mg/kg PAP and 200 mg/kg HCBD. See text for experimental conditions. *cn*, creatinine; *2-OG*, 2-oxoglutarate; *tau*, taurine.

means of standard function-minimization techniques. PCA is a well established statistical technique for dimension reduction (32, 33). PCs are linear combinations of the original variables with appropriate weighting coefficients. The properties of these PCs are such that (i) each PC is orthogonal (uncorrelated) with all other PCs and (ii) the first PC contains the largest part of the variance of the data set (information content), with subsequent PCs containing correspondingly smaller amounts of variance. Thus, a plot of the first and second PCs, which may have negligible contributions from some of the input parameters, gives a selective but maximal representation in terms of information content of the data. We have found it useful to display three-dimensional PCA plots to increase the information content (i.e., orthogonal plots of the first three principal components); these are depicted here as stereo diagrams, for viewing using a standard stereoscope.

Correlation coefficients (r) were also calculated based on the relationship between parameters, and correlation matrices were generated. Each matrix is a table, with toxins along the top and down the left side, in the same order, such that the diagonal elements always have a value of 1.0 and all other values reflect intertoxin correlations. From this are calculated the coefficients (r^2) of the square correlation matrix, from which was subtracted the overall mean, thus providing scaled data for use in further NLM and PCA studies. Such 'correlation maps' were not autoscaled. All correlation maps shown in this work are of this latter type. Maps calculated based on r itself rather than r^2 provided similar clustering, but with slightly more dispersed clusters. It is important to note that the method adopted does not distinguish between anticorrelation and correlation. However, we observed that there was little appreciable anticorrelation in the NMR-generated toxicological data considered in this work.

Results

NMR spectroscopy of urine from toxin-treated rats. Typical ^{1}H NMR spectra obtained from rat urine samples after exposure to various nephrotoxins and hepatotoxins are shown in Figs. 1, 2, and 3. Hg and HCBD cause toxicity to the pars recta of the proximal tubule and produce reproducible patterns of change in urinary low molecular weight metabolites, particularly elevations in alanine, glutamine, lysine, valine, glucose, and L-lactic acid. Although the NMR patterns obtained for HCBD and Hg (which have similar time courses of toxic action and identical nephronal region specificity) have some common features, they are substantially different both qualitatively and quantitatively (Fig. 1), reflecting differences in the mechanisms of action of the toxins on the proximal tubular epithelium. The NMR spectra reveal that the pattern of urinary metabolites after exposure to a renal papillary toxin is dissimilar to that seen after exposure to the proximal tubular toxins (Fig. 1). For instance, 2 days after a nephrotoxic dose of BEA, rats excrete increased amounts of acetate, succinate, DMG, and DMA (effects are evident within 8 hr) (Fig. 1). It would appear that, when two different toxins act on the same region of the nephron, the pars recta of the proximal tubule, and have very similar mechanisms of action, as in the case of PAP and HCBD (6,

TABLE 2

Scored data obtained from NMR spectra of urine after exposure to organ-specific toxins

This table is a condensed representation of the effects of the toxins on the urinary profiles of low molecular weight metabolites for the post-dosing period to 24 h after dosing. A, Data for the training set of 10 toxins; B, the test set. See Experimental Procedures for a description of the scoring system used. Data from animals receiving UN, ALY, PAP (50 mg/kg), Hg, and Cd were used to test the classifications derived from the training set of 10 toxins. The urinary metabolites were: Ace, acetate; Ala, alanine; HB, 3-D-hydroxybutyrate; Cit, citrate; Cn, creatinine; Cr, creatine; Glc, glucose; Gln, glutamine; Hip, hippurate; Lac, lactate; 2-OG, 2-oxoglutarate; Suc, succinate; Val, valine; Lys, lysine; Tau, taurine. F, Female. Numbers in parentheses, dose.

A.	Hg (fed)	PAP (100)	CrO_4	HCBD	PI	BEA	HYD	CCl_4	ANIT	THIO
Ace	1	1	1	1	3	2	3	0	2	0
Ala	1	2	1	2	1	1	0	0	0	0
HB	0	1	0	1	0	0	0	0	0	0
Cn	−1	−1	−1	0	0	0	0	−1	0	−1
Cit	−3	−2	0	0	1	−2	−2	−2	−2	−2
Glc	2	3	3	3	1	1	0	0	1	0
Gln	1	2	2	2	0	0	0	0	0	0
2-OG	−2	−1	−1	−1	−2	−3	−2	−2	−2	0
Hip	−1	−1	−2	−3	0	−1	0	−1	0	−2
Lac	3	3	1	3	1	1	2	0	1	0
Suc	−3	1	−1	1	3	2	−2	−2	2	−2
TMAO	−2	0	0	0	−3	−3	0	−1	0	−1
Val	1	2	0	2	0	0	0	0	0	0
DMA	−1	0	0	0	2	2	−1	−1	0	−1
Lys	1	2	1	2	0	0	0	0	0	0
Tau	0	0	0	0	0	0	3	3	3	3
DMG	0	0	0	0	3	3	0	0	0	0
Cr	0	0	0	0	0	2	0	0	0	0

B.	ALY	UN	PAP (50)	Hg (0.5)	Hg (1.0)	Hg (1.5)	Hg (2.0)	Cd (6)	Cd (9)	Cd (12)	Cd (24)	Cd (F)
Ace	3	0	1	−1	1	2	3	0	0	0	1	0
Ala	1	0	2	0	3	3	3	0	0	0	0	0
HB	0	3	1	2	3	3	3	0	0	1	1	0
Cn	0	−2	−1	0	0	−2	−2	0	0	0	0	0
Cit	−1	−3	−1	−2	−2	−3	−3	0	−2	−2	−2	−2
Glc	0	3	2	0	2	3	3	0	0	0	0	0
Gln	0	2	1	0	2	2	2	0	0	0	0	0
2-OG	−2	−3	−1	−2	2	2	3	0	−1	−1	−1	−2
Hip	0	−3	−1	−1	0	−1	1	−1	−1	−1	−2	−1
Lac	2	2	2	−2	2	2	3	0	0	0	0	0
Suc	3	−2	1	−1	1	1	3	−1	−1	−1	−2	−2
TMAO	−2	−2	0	0	2	2	3	0	0	0	0	0
Val	0	1	1	0	2	2	3	0	0	0	0	0
DMA	0	−2	0	0	0	−2	−2	0	0	0	0	0
Lys	0	1	1	0	0	1	1	0	0	0	0	0
Tau	1	0	0	0	0	0	0	0	0	0	1	0
DMG	−3	0	0	0	0	−2	0	0	0	0	0	0
Cr	0	0	0	0	0	0	0	0	3	3	3	2

35), the NMR urinalysis patterns are strikingly similar (Fig. 3), although detailed examination reveals that PAP causes a decrease in urinary citrate, whereas HCBD does not (see also Table 2). When toxins cause damage to the liver, further substantial differences in urinary composition occur. In particular, acute liver injury is associated with high levels of taurine in the urine, as is shown for HYD in Fig. 2 and as is also true of ANIT, CCl_4, and THIO (18).

NMR data scoring. Data were gathered from a large number of urinalysis spectra obtained from many individual animals at various time points after exposure to toxins, and individual metabolite signals were identified and scored according to their intensity (corrected for urinary volume and vertical scale expansion), as presented in Tables 2–4. In typical 400-MHz ^1H NMR spectra from rat urine, the ability to detect and assign 30–50 different metabolites is common, under the spectral acquisition conditions used (4). Initially, we chose to use a smaller number of metabolites for PR purposes, i.e., 17 that are detectable in all control rat urine samples and for which full use of the proposed seven-level scoring system can be made in all cases. For instance, slight elevations in urinary histidine and tyrosine concentrations were seen after HCBD-induced nephrotoxicity (Fig. 1C), and increased urinary formate concentration was observed in the case of CrO_4-induced nephrotoxicity (Fig. 1B). These components are usually not present in significant quantities in control urine or are highly variable, and they were not considered reliable markers or descriptors in our primary PR analysis. Table 2A contains scored information on the effects of 10 toxins on the excretion patterns of the 17 chosen metabolites, representing the maximal change in metabolite concentration occurring in a 24-hr period after dosing. Table 3 contains scored information on the changes in 16 metabolite concentrations (all of the above except taurine, which displayed no effect) occurring at three time points after administration of six nephrotoxins, i.e., each toxin is now represented by a 48-dimensional metabolic space, with three time-point dimensions per metabolite. Taurine is not scored in this table (or used in subsequent analysis) because none of the

TABLE 3

Scored data for 16 metabolites (as in legend to Table 2 but without taurine, because its excretion is not altered by any nephrotoxin in the current list), throughout three time periods, 0–8 hr, 8–24 hr, and 24–48 hr, obtained from NMR spectra of urine that was collected after exposure to six nephrotoxins

See Experimental Procedures for a description of the scoring system used. See legend to Table 2 for list of abbreviations.

	Hg (fed)	PAP	CrO_4	HCBD	PI	BEA
Ace	0,1,1[a]	1,1,1	0,0,1	0,1,1	1,2,3	1,2,2
Ala	0,1,1	2,2,2	0,0,1	0,2,2	0,1,1	0,1,1
HB	0,0,0	1,1,1	0,0,0	0,1,1	0,0,0	0,0,0
Cn	−1,−1,−1	−1,−1,−1	−1,−1,−1	0,0,0	0,0,0	0,0,0
Cit	−1,−2,−3	−1,−1,−2	0,0,0	0,0,0	0,0,1	0,−1,−2
Glc	0,2,2	2,3,3	0,0,3	0,3,3	0,0,1	0,0,1
Gln	0,1,1	1,2,2	0,0,2	0,2,2	0,0,0	0,0,0
2-OG	−1,−2,−2	−1,−1,−1	0,0,−1	−1,0,−1	0,0,−2	0,−3,−3
Hip	0,0,−1	−1,−1,−1	0,0,−2	−1,−1,−3	0,0,0	0,0,−1
Lac	0,2,3	2,2,3	0,0,1	0,2,3	0,1,1	0,1,1
Suc	0,−1,−3	1,−1,1	0,0,−1	0,0,1	−1,2,3	−1,1,2
TMAO	−1,−1,−2	0,0,0	0,0,0	0,0,0	2,2,−3	2,−3,−3
Val	0,1,1	1,2,2	0,0,0	0,2,2	0,0,0	0,0,0
DMA	0,−1,−1	0,0,0	0,0,0	0,0,0	2,2,1	2,2,1
Lys	0,1,1	1,2,2	0,0,1	0,2,2	0,0,0	0,0,0
DMG	−1,−1,0	1,0,0	0,0,0	−1,−1,0	0,0,3	0,0,3

[a] Scores are given for the three time periods studied.

TABLE 4

Scored data for 16 metabolites (as in legend to Table 2 but without taurine) obtained, using a double-scoring system (time of maximum change and magnitude of change, from NMR spectra of urine that was collected after exposure to six nephrotoxins

See Experimental Procedures for a description of the scoring system used. See legend to Table 2 for list of abbreviations.

	Hg (fed)	PAP	CrO_4	HCBD	PI	BEA
Ace	2,1[a]	1,1	3,1	2,1	3,3	2,2
Ala	2,1	1,2	3,1	2,2	2,1	2,1
HB	0,0	1,1	0,0	2,1	0,0	0,0
Cn	1,−1	1,−1	1,−1	0,0	0,0	0,0
Cit	3,−3	3,−2	0,0	0,0	3,1	3,−2
Glc	2,2	2,3	3,3	2,3	3,1	3,1
Gln	2,1	2,2	3,2	2,2	0,0	0,0
2-OG	2,−2	1,−1	3,−1	1,−1	3,−2	2,−3
Hip	3,−1	1,−1	3,−2	3,−3	0,0	3,−1
Lac	3,3	3,3	3,1	3,3	2,1	2,1
Suc	3,−3	1,1	3,−1	3,1	3,3	3,2
TMAO	3,−2	0,0	0,0	0,0	3,−3	2,−3
Val	2,1	2,2	0,0	2,2	0,0	0,0
DMA	2,−1	0,0	0,0	0,0	1,2	1,2
Lys	2,1	2,2	3,1	2,2	0,0	0,0
DMG	1,−1	1,1	0,0	1,−1	3,3	3,3

[a] Scores are given for time of maximum change and magnitude of change.

nephrotoxins examined alters taurine excretion and by definition all scores are, therefore, zero. Table 4 shows an alternative approach to scoring the time-course data for nephrotoxins, where two scores are given per metabolite, the first being the maximal excretion change score (indicating the biggest change that occurs at any of the three time points) and the second being a score for the time at which this change occurs (i.e., 1, 2, or 3, corresponding to the first, second, or third time point at which the maximal change occurs). This table should, therefore, carry most of the information present in Table 3, in only 32 dimensions. Table 5 contains the Euclidean interpoint distances between the toxins, in terms of both the original 17-dimensional metabolite space, calculated from Table 2, and the two-dimensional metabolite space representative of the NLM.

Classification of NMR data on training set toxins by PR methods. HCA was chosen as a preliminary method of analyzing the scored NMR data. HCA involves the calculation of a similarity index that reflects the n-dimensional urinary metabolite interpoint distances, using the selected 17 metabolic dimensions listed in the legend to Table 2. In the cluster dendrogram (Fig. 4), the four hepatotoxins form a discrete cluster, with CCl_4, THIO, ANIT, and HYD appearing similar within the cluster; all proximal tubular toxins form a cluster, with PAP and HCBD being the most similar. The papillary toxins PI and BEA are also closely associated and in turn are marginally closer to hepatotoxins than to the cortical nephrotoxins.

In the two-dimensional NLM (Fig. 5A), three subspaces of "biological activity" can be seen, based on site or organ of toxicity. The four proximal tubular toxins, papillary toxins, and centrilobular hepatotoxins tend to group in different zones of the map (Fig. 5A), although CrO_4 and Hg are as close to the hepatotoxins as they are to the papillary nephrotoxins. We have tested whether NLMs produce major distortions in the displayed clusters, by calculating interpoint distances both in the full multidimensional parameter space and in the two-dimensional NLM space. From Table 5 it can be seen that the relative distances are largely preserved. NLMs incorporate all of the variance present in the metabolite input data set (including data noise), whereas the PC maps incorporate only the major fraction of the variance into two- or three-dimensional diagrams, with these proportions varying from data set to data set, but some data noise is eliminated.

PC analysis of these data produced more discrete clustering than seen in the NLMs, with toxin subclusters being better defined (Fig. 5B). HCBD and PAP are shown close together in the NLM but closer in the PC map (Fig. 5B). PI and BEA, toxins that produce renal papillary necrosis, are very close in the PC map but are far removed from the hepatotoxins and the other nephrotoxins (Fig. 5B). We have found that taking the coefficients of determination (r^2) between toxins as parameters to generate so-called 'correlation maps' results in improved clustering in both NLM and PC analysis. Here, toxins fall into three discrete clusters of biological activity, proximal tubular toxins, renal papillary toxins, and hepatotoxins (Fig. 5, C and D). ANIT, although clearly part of the hepatotoxin cluster, is slightly separated from the other three hepatotoxins, possibly reflecting its differing site of primary toxicity (intrahepatic cholestasis rather than centrilobular damage) (Fig. 5D).

In data matrices of the type described here, it is possible that a significant amount of biological information may be carried in the third (or possibly even fourth) PCs or that situations may arise in which PC2 and PC3 are very similar in terms of variance content. In these circumstances, these data can be better examined by displaying a three-dimensional PC in the form of a stereo pair of diagrams; this method of display was only recently introduced (34). The three-dimensional PC map of the toxins in metabolite space, calculated from the data in Table 2A (see Fig. 8A), shows Hg and CrO_4 to be well separated, suggesting that a significant amount of information is contained in the third PC of this data set and indicating that there are significant differences in the biochemical response to these toxins, as expected by their sites of action. This was confirmed by examination of the distribution of the data set variances between the first three PCs, which correspond to 42, 32, and 10%, respectively. The three-dimensional PC map thus gives superior discriminatory power in the classification of toxicity type over the two-dimensional representations and might be

TABLE 5

Interpoint distances between toxins in *n*-dimensional space (above diagonal) and two-dimensional space (compressed from *n*-space; below diagonal), calculated from the data set listed in Table 2A

	Hg (fed)	PAP	CrO_4	HCBD	PI	BEA	HYD	CCl_4	ANIT	THIO
Hg (fasted)	**0.0**	1.58	1.44	1.92	2.32	1.96	1.65	1.53	1.77	1.76
PAP	1.23	**0.0**	1.56	1.16	2.47	2.34	2.37	2.35	2.22	2.37
CrO_4	1.04	1.20	**0.0**	1.60	2.06	2.03	1.93	1.67	1.77	1.63
HCBD	1.97	1.04	1.27	**0.0**	2.59	2.54	2.53	2.58	2.39	2.51
PI	2.59	2.63	1.61	2.02	**0.0**	1.01	1.97	2.21	1.67	2.42
BEA	2.51	2.93	1.75	2.59	0.85	**0.0**	1.84	1.90	1.53	2.23
HYD	1.41	2.21	1.09	2.32	1.64	1.22	**0.0**	1.33	0.85	1.65
CCl_4	1.49	2.65	1.81	3.07	2.61	2.07	0.98	**0.0**	1.26	0.86
ANIT	2.01	2.88	1.74	2.94	1.84	1.13	0.67	1.02	**0.0**	1.60
THIO	1.09	2.32	1.81	2.97	3.01	2.61	1.41	0.73	1.68	**0.0**

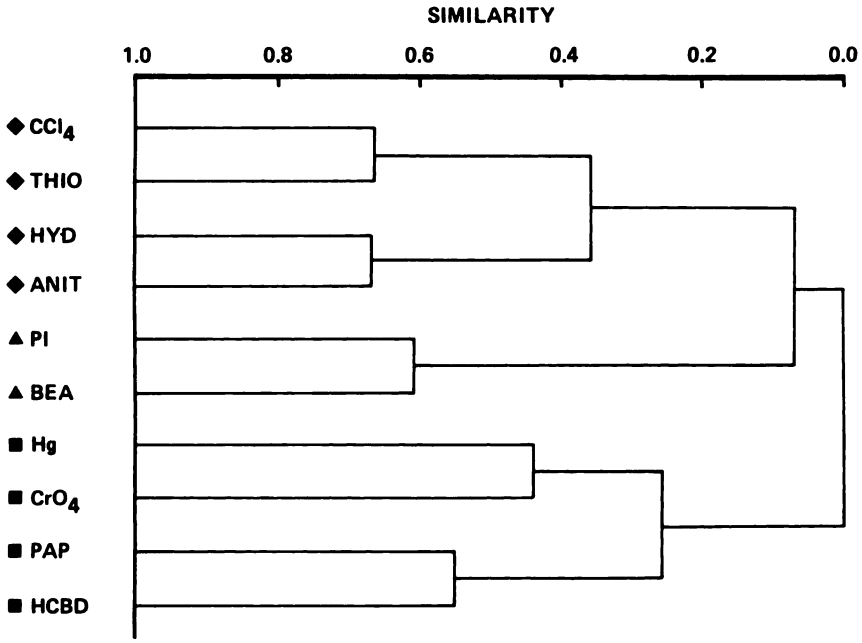

Fig. 4. Connection dendrogram produced by the HCA routine (centroid method) housed within the PR package ARTHUR, showing the 10 toxins (training set) on a similarity scale of 0 to 1 (0 = most dissimilar and 1 = most similar). Input data were the same as those used to generate Fig. 5, A and B (toxins mapped in metabolite space). Data were autoscaled before analysis.

expected to be more useful in situations in which a wide range of biochemical responses are being mapped simultaneously (see Fig. 8B).

The effect of application of different data-scoring methods to the nephrotoxin training subset on apparent clustering in NLMs and PCs was tested, and the results are shown in Fig. 6. All maps in this figure are correlation maps derived from 16 dimensions (Fig. 6, A and B, maximal change after exposure), 48 dimensions (Fig. 6, C and D, three time points for each metabolite), and 32 dimensions (Fig. 6, E and F, one time point descriptor showing time of maximal change for each metabolite), corresponding to the scores listed in Tables 2A, 3, and 4, respectively. The overall clustering pattern is preserved in all the NLMs and PC maps, and in all cases proximal tubular and papillary toxins were discriminated. However, as might be expected, the three-point time-course scoring data (which have the highest original dimensionality) seem to offer the best representation, in that the proximal tubule pars convoluta toxin (CrO_4) is discriminated from the pars recta toxins (Hg, PAP, and HCBD) (Fig. 6C). Significantly improved (tighter) clustering is seen in all PC maps over NLMs displayed in Fig. 6. The basic pattern of clustering seen in the PC maps is preserved irrespective of the scoring system used, but CrO_4 is best separated from the other proximal tubular toxins by inclusion of the time-course information.

PR analysis of combined training and test set data and classification of toxins by NMR PR methods. PC maps provide consistently better clustering and classification of the training set data, and hence the effect of the addition of test set data was evaluated and illustrated using PC analysis. The effect of the progressive addition of test set data to the original training set data (Fig. 5D) on clustering in correlation PC maps is shown in Fig. 7. Addition of NMR urinalysis data on the nephrotoxins UN and Hg (in the fasted state, with dose-response information) and the hepatotoxin ALY to the training set results in the appearance of four discrete toxin clusters, i.e., papillary toxins, proximal tubular toxins (fed animals), Hg (fasted animals), and hepatotoxins (Fig. 7A). However, the cluster of points from the fasted, Hg-treated animals should be considered as a satellite to the main proximal tubular toxin cluster. Interestingly, the lowest dose of Hg [which was not nephrotoxic but produced some minor perturbations in urinary composition (1)] given to fasted animals falls near ALY, suggesting similarity in terms of input parameters. In fact, both of these points map close to the theoretical 0,0 coordinate in the PC map that is expected for a control animal. Addition of dose-response data from another chemical with quite distinct target organ toxicity, Cd, a testicular toxin that also causes RCA inhibition in both male and female rats (8), resulted in the map

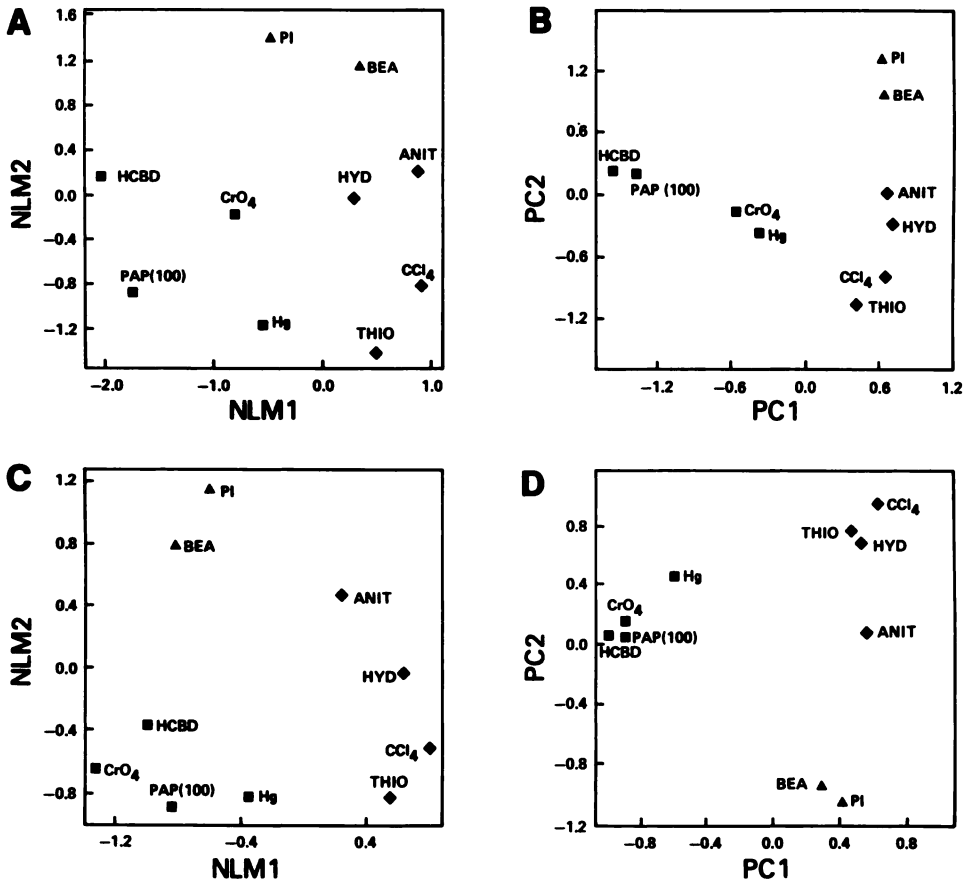

Fig. 5. Nonlinear maps (A and C) and plots of the first two PCs (B and D) for the NMR-derived training data set, displaying toxins mapped in metabolite space (A and B) and in correlation space (C and D). Values for the first three PCs are PC1 = 41%, PC2 = 31%, and PC3 = 10% (B) and PC1 = 43%, PC2 = 40%, and PC3 = 7% of the total variance (D). Data used to generate A and B were autoscaled before analysis, whereas data used to generate C and D were not autoscaled. All parameters were equally weighted. In each space, the PC map manifested tighter clustering than that seen in the NLM. Maps in correlation space show improved clustering over the corresponding maps derived from the original data.

shown in Fig. 7B. Although inverted about PC1, the overall pattern of clustering and the intracluster relationships are well preserved. Further, the Cd data produce a discrete cluster of data points, with only the lowest dose [6 μmol/kg, which does not cause acute toxicity or RCA inhibition (8)] mapping distant to the points marking the higher doses of Cd. The addition of another metabolic dimension, urinary creatine, a known marker of testicular toxicity (8), to the data set that generated Fig. 7B produced Fig. 7C. Again, discrete clusters of organ-specific toxins are apparent, with ANIT, ALY, BEA, and PI being more clearly discriminated than in Fig. 7B. The points describing the effects of the metal nephrotoxins UN and Hg (2 mg/kg in fed animals) remain close in all maps shown in Fig. 7, reflecting strong similarities in the effects of the toxins on the urinary profile of low molecular weight components. The representative three-dimensional correlation PC map that is equivalent to the two dimensional map in Fig. 7C is shown in Fig. 8B. ANIT and BEA, apparently close in Fig. 7C, are separated by the third PC, with ANIT mapping in the background and PI and BEA mapping in the foreground in Fig. 8B (i.e., the renal papillary toxicity is distinguished and classified by the third PC in this extended data set). The third PC also succeeds in separating the hepatotoxin group (HYD, THIO, and CCl_4) from the low dose (nontoxic) Hg and Cd treatments, which are also apparently close in Fig. 7C. Other third PC separations include Cd_{12} (12 μmol/kg Cd) from the other Cd doses, Hg_1 (1 mg/kg in fasted animals) from the other Hg doses, and Hg (2 mg/kg in fed animals) from UN. Comparison of Fig. 7, B and C, also reveals that, although the presence of the specific marker creatine helps to differentiate Cd from other toxins, even without this the information carried in the other metabolic dimensions is sufficient to provide a clear separation. The results clearly show that a significant amount of information is contained in the third PC of this data set. This was confirmed by examination of the distribution of the data set variances between the first three PCs, which correspond to 39, 21, and 14% (Fig. 8B), respectively. The fact that male and female rats were not readily discriminated despite the testicular toxicity of Cd is a consequence of the masking effect of the RCA inhibition, which affects several descriptors (e.g., succinate, 2-oxoglutarate, and citrate), whereas testicular toxicity *per se* affects only urinary creatine. Furthermore, the particular scoring system used does not take into account the very much greater effect of Cd on urinary creatine that occurs in males over females (8).

Application of HCA to the combined training and test set data produced the dendrogram shown in Fig. 9. All proximal tubular toxins form a cluster, within which is sited a subcluster consisting of the fasted Hg doses that produced a toxic effect. Hepatotoxins form two discrete clusters, which are far removed from each other, with the ANIT-ALY cluster being more similar to the papillary toxins than to the other hepatotoxins (Fig. 9). All toxic doses of Cd (9–24 μmol/kg) form a cluster within the dendrogram, with the 'no-effect' doses of Cd (6 μmol/kg) and Hg (0.5 mg/kg; fasted) appearing similar in effects (Fig. 9).

Discussion

Biological significance of toxicological data carried by NMR spectra of urine. ^1H NMR spectra of biofluids are all very rich in information, which is carried in the overall pattern of the metabolite resonances (9). For instance, most nephrotoxins produce characteristically different spectral patterns of

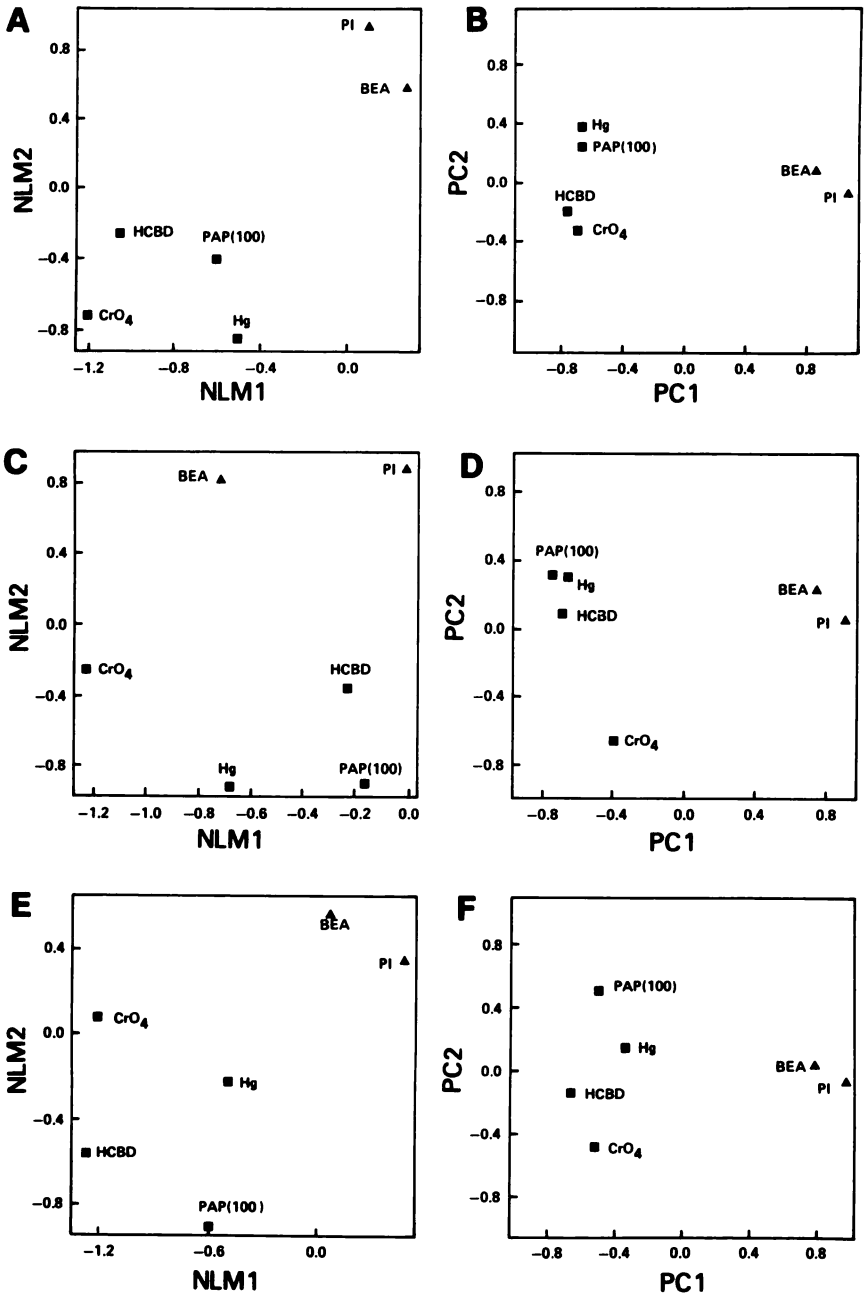

Fig. 6. Nonlinear maps (A, C, and E) and plots of the first two PCs (B, D, and F) of the ^{1}H NMR data set, displaying nephrotoxins alone mapped in the correlation space. A and B, These plots, respectively, from the overall data set; C and D, the time-course data set; E and F, result of a dual-scoring system (see Table 4). Data were not autoscaled before analysis. Values for the first three PCs are PC1 = 85%, PC2 = 8%, and PC3 = 4% (B); PC1 = 69%, PC2 = 17%, and PC3 = 7% (D); and PC1 = 70%, PC2 = 14%, and PC3 = 11% (F) of the total variance. *PAP (100)*, PAP at 100 mg/kg.

urinary metabolites (Fig. 1). Descriptions of the perturbed NMR spectral patterns of rat urine after exposure to CrO_4, PAP, HCBD, Hg, BEA, PI, and HYD have been reported previously (3–5). Proximal tubular toxins commonly cause glycosuria, aminoaciduria, and L-lactic aciduria, whereas renal papillary toxins cause early elevations (within 8 hr) in urinary DMA and TMAO, with later elevations (24–48 hr) in DMG, acetate, and succinate and a decrease in TMAO (1, 4, 5). The close similarity in the patterns observed in the ^{1}H NMR spectra of urine from rats exposed to PAP and HCBD is striking (Fig. 2). This is of particular interest because both toxins produce damage to the same segment of the proximal tubule, i.e., the pars recta (5, 12), and recent NMR and conventional biochemical studies have shown that both PAP and HCBD share a common site and mechanism of toxicity involving the generation of a hepatic glutathione-derived toxic thiol conjugate (6, 35). This implies that, in addition to information that identifies sites and biochemical action of toxins, ^{1}H NMR data from biofluids may also have predictive value in identifying mechanisms of action of poorly understood or novel toxins. The hypothesis that this similarity in pattern merely reflects the end stage of the toxicological process is rejected because, for instance, Hg and PAP damage the same region of the proximal tubule over a similar time course but have very different biochemical mechanisms of toxicity and, hence, different ^{1}H NMR urinalysis patterns. PAP and HCBD, on the other hand, have similar toxic mechanisms (6, 35) and produce similar ^{1}H NMR urinalysis profiles (Fig. 3), as exemplified by the PR analysis (Figs. 5 and 9). More recently, we have shown that the ^{1}H NMR urinalysis profile after exposure to 40 mg/kg *S*-(1,2-dichlorovinyl)-L-homocysteine, a chemical that also produces nephrotoxicity via a mechanism similar to that of PAP and HCBD (36), closely resembles those seen after both HCBD and

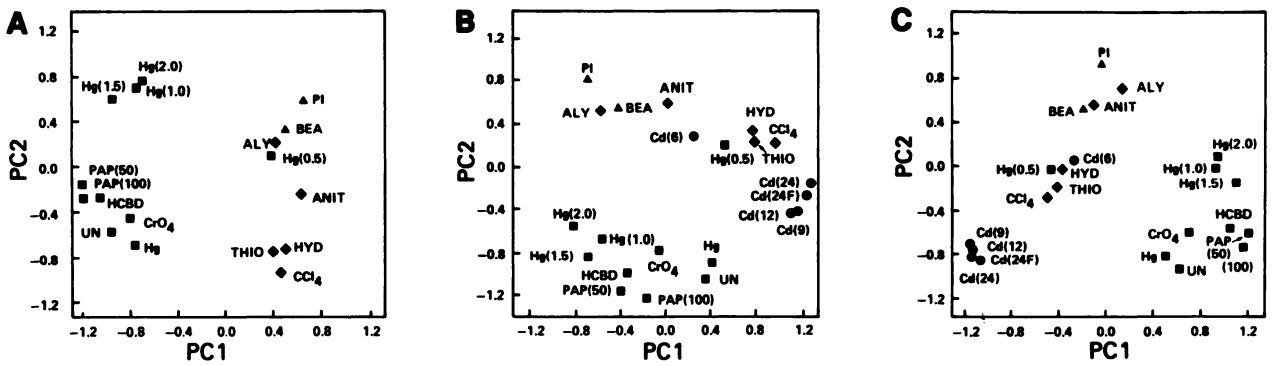

Fig. 7. Plots of the first two PCs of the combined training and test set data mapped in the correlation space. A, Training set after the addition of data obtained from fasted rats receiving increasing doses of Hg, the periportal hepatotoxin ALY, and the proximal tubular toxin UN. B, Map A after addition of data obtained from rats receiving increasing doses of Cd (F, female). C, Map B after addition of another dimension, creatine, to the data set. Data were not autoscaled before analysis. Values for the first three PCs are PC1 = 42%, PC2 = 22%, and PC3 = 15% (A); PC1 = 32%, PC2 = 30%, and PC3 = 12% (B); and PC1 = 39%, PC2 = 21%, and PC3 = 14% (C) of the total variance. *Numbers in parentheses*, dose (refer to Table 1).

PAP but with a time-course identical to that of PAP, i.e., toxicity is seen within 8 hr of exposure.[1]

Whereas it is apparent that a contribution to the subclustering seen in the fasted Hg-treated group of rats arises from the fasting state, any effects arising from differences in rat strain cannot be ruled out as discriminatory factors, and these should be considered. The Fischer 344 rat is well known to be sensitive to nephrotoxic agents (4–6). Indeed, this animal is commonly used in mechanistic nephrotoxicity studies (6, 37). The Sprague-Dawley rat, on the other hand is not considered to be particulary sensitive to nephrotoxic insult; this strain displays a degree of resistance to the nephrotoxic effects of PAP due to a high hepatic *N*-acetyltransferase activity that converts PAP to paracetamol, a detoxification step (38). Thus, it is vital to consider strain differences in sensitivity/resistance to toxicity when interpreting such data.

Data scoring. The PR methods described have been applied to data that have been scored based on an arbitrary system. Three different approaches to scoring have been demonstrated, all of which produce similar PR maps (both NLM and PC), indicating that the arbitrary system selected is reasonably robust. The greatest discriminatory capability, not surprisingly, is displayed by the scoring system that has the most information in the starting data set, i.e., the three-point time course (Table 3); however, only marginally inferior results were obtained with reduced data sets such as the dual excretion-time system (Table 4) or even the system employing the maximal change criteria, which contains no real time-course data (Table 2). The implication is that NMR provides, at least for the toxins considered here, an excess of information needed for toxicity classification by PR methods. For more complex biological scenarios involving, for instance, dose-response classifications, nutritional influences on biochemical manifestations of toxic lesions, and toxins producing effects on other organ systems, the scoring system based on these 17 metabolites may not be overdefined.

Evaluation of PR methods. If NMR urinalysis data are to be useful in the prediction of toxicity, the PR analysis data for a training set of compounds must give a discrete classification of toxicity type that is generally robust to addition of novel data types, including new metabolic descriptors and new toxin classes. The results obtained from the HCA routine are reliable in that discrete clusters of proximal tubular toxins, renal papillary toxins, and hepatotoxins are clearly visible (Fig. 4). Even within these clusters, this method provides predictable results; PAP and HCBD, two proximal tubular toxins with similar mechanisms of toxicity, form a subcluster (Fig. 4). The results obtained from the HCA routine agree very closely with those obtained using the NLM method. This is most clearly demonstrated in Figs. 4 and 5A for toxins mapped in metabolite space and is preserved when using the correlation method, as can be seen by comparing Figs. 7C and 9. NLMs contain all of the information present in the original data set and give an indication of the strength of the associations between the different toxins in metabolic terms. However, because they represent least-squares fits to the true Euclidian interpoint distance in *n*-space, they are distorted data compressions and, hence, may give anomalous results. PCA, on the other hand, gives an exact mathematical solution, and PC maps appear to give superior results, in terms of toxin type discrimination, to those of NLMs. However, the importance of maintaining the variance proportion as high as possible in relation to the content of the original data set is emphasized by the superior discriminatory ability and separation of toxin classes given by the three-dimensional PC maps. These three-dimensional maps will probably be most useful when a large number of toxin types or a wide range of metabolic descriptors are being used, as is likely in situations in which novel therapeutic agents are being screened for toxic side effects as part of a drug development program. Our investigations lead us to believe that PC maps probably do not give a useful representation of the Euclidean interpoint distances (and hence meaningful classification of the data) unless at least 75% of the original input data set variance is displayed in the data compression. Correlation maps appear to offer superior results in terms of tightness of clustering and maximization of intercluster distances. This is to be expected, because biochemical effects are dose dependent; in the comparison of one toxin at different doses or two related toxins at arbitrary doses, the magnitudes of the effect may differ (thus separating points in the metabolite hyperspace), even though the trends may be similar.

Concluding remarks. In the present study, we have used scored data derived from inspection of changes in NMR peak intensities after exposure to seven nephrotoxins, five hepato-

[1] Unpublished observations.

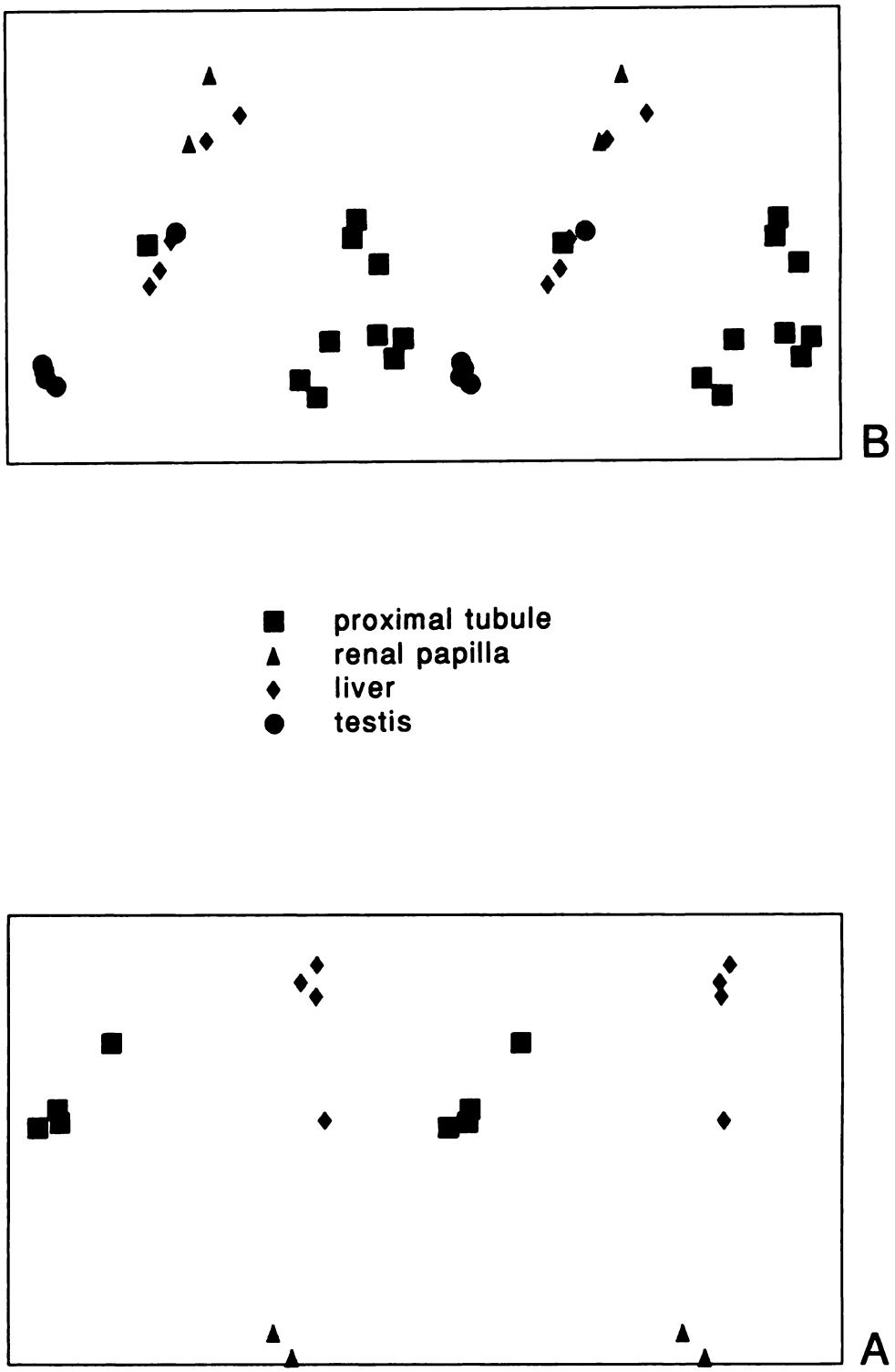

Fig. 8. Three-dimensional stereo pair PC maps of the 10 toxins (training set) (A) and the 22 toxins (combined training and test sets) (B), displaying toxins mapped in the correlation space. The *x*-, *y*-, and *z*-axes represent the first, second, and third PCs, respectively. Data were not autoscaled before analysis. Values for the first three PCs are PC1 = 43%, PC2 = 40%, and PC3 = 7% (A); and PC1 = 39%, PC2 = 21%, and PC3 = 14% (B) of the total variance. For keys to labels for A see Fig. 5D and for B see Fig. 7C. *Red square*, proximal tubular toxin; *green triangle*, renal papillary toxin; *blue diamond*, hepatotoxin; *magenta circle*, Cd.

toxins, and one compound causing renal tubular acidosis and testicular toxicity. This was carried out with a view to testing the validity of using PR methods in the analysis of NMR data and is seen as a prelude to a more direct means of NMR spectral analysis, involving transfer of peak integral data tables from the associated spectrometer computer (ASPECT 3000) to that housing the PR software (VAX 8550). An important step in this regard was the use of "new" data to test the derived classifications.

NMR itself provides a simple and elegant method for detect-

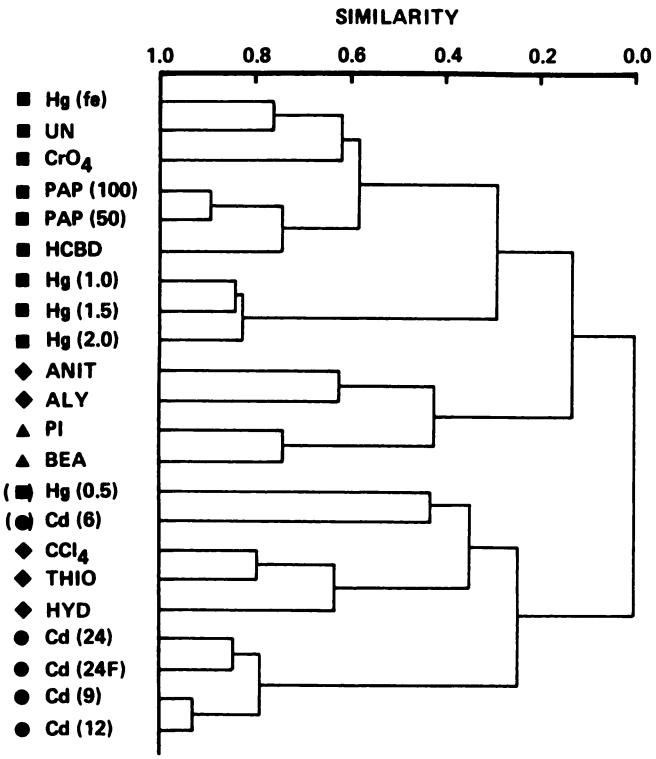

Fig. 9. Connection dendrogram produced by the HCA routine (centroid method) housed within the PR package ARTHUR, showing the 22 toxins (training set and test set) on a similarity scale of 0 to 1 (0 = most dissimilar and 1 = most similar). *Parentheses*, subtoxic dose. Input data were the same as those used to generate Fig. 7C (toxins mapped in correlation space). Data were not autoscaled before analysis.

ing and monitoring toxicity through body fluid analysis. However, the complexity of biofluid ^{1}H NMR spectra requires that considerable care be taken in the interpretation and analysis steps, in order to extract meaningful biological data, and this approach to toxicological assessment is still at an early stage of development. These PR methods provide an efficient means of reducing the potentially enormous NMR urinalysis data set to interpretable proportions, and provide a means of classifying toxicological data using a large number of metabolic dimensions. The utility of these methods will become more apparent when considering the complexity of 600 MHz spectra of biofluids, which may contain about an order of magnitude more information than an equivalent 400 MHz spectrum recorded on the same biological sample. At present, we are applying the combined PR and ^{1}H NMR approach to urine and other body fluids and tissue extracts, in an attempt to identify additional novel low molecular weight metabolic markers of tissue injury. In addition, we are exploring the possibility of using more conventional markers of tissue injury in our studies, for example, histology and urinary enzymes, in an attempt to further classify toxicity. ^{1}H NMR-based toxicological methods should, at least for the present time, be regarded as a novel means of supplementing conventional toxicity data. The PR-^{1}H NMR approach shows considerable promise in toxicology; it could be of great value in the screening of novel drugs for acute side effects at an early stage of their development and, hence, could contribute to a reduction in the use of laboratory animals for toxicological testing. In addition, NMR methodology could be used to monitor the recovery phase from reversible toxic insult or disease states and, in the latter case, might also provide a novel means of monitoring therapy.

Acknowledgments

We thank F. W. Bonner, J. A. Timbrell, M. Anthony, S. Sanias and E. Rahr for their advice and technical assistance, S. Moncada, F.R.S., for encouragement and support, and The Wellcome Foundation and The National Kidney Research Fund for financial support of this and related work. We thank the Medical Research Council for use of central NMR facilities.

References

1. Nicholson, J. K., J. A. Timbrell, and P. J. Sadler. Proton NMR spectra of urine as indicators of renal damage: mercury-induced nephrotoxicity in rats. *Mol. Pharmacol.* **27**:644–651 (1985).
2. Bales, J. R., J. D. Bell, J. K. Nicholson, P. J. Sadler, J. A. Timbrell, R. D. Hughes, P. N. Bennett, and R. Williams. Metabolic profiling of body fluids by proton NMR: self-poisoning episodes with paracetamol (acetaminophen). *Magn. Res. Med.* **6**:301–306 (1988).
3. Sanins, S. M., J. A. Timbrell, C. Elcombe, and J. K. Nicholson. Proton NMR studies on the metabolism and biochemical effects of hydrazine *in vivo*, in *Methodological Surveys in Biochemistry and Analysis* (E. Reid and I. D. Wilson, eds.), Vol. 18. Plenum Press, New York, 375–381 (1988).
4. Gartland, K. P. R., F. W. Bonner, and J. K. Nicholson. Investigations into the biochemical effects of region-specific nephrotoxins. *Mol. Pharmacol.* **35**:242–250 (1989).
5. Gartland, K. P. R., F. W. Bonner, J. A. Timbrell, and J. K. Nicholson. The biochemical characterisation of *p*-aminophenol-induced nephrotoxic lesions in the F344 rat. *Arch. Toxicol.* **63**:97–106 (1989).
6. Gartland, K. P. R., C. T. Eason, F. W. Bonner, and J. K. Nicholson. The effects of biliary cannulation and buthionine sulphoximine pretreatment on the nephrotoxicity of *para*-aminophenol in the Fischer 344 rat. *Arch. Toxicol.* **64**:14–25 (1990).
7. Gartland, K. P. R., K. E. Wade, C. T. Eason, F. W. Bonner, and J. K. Nicholson. Proton NMR spectroscopy of bile for monitoring the excretion of endogenous and xenobiotic metabolites: application to *p*-aminophenol. *J. Pharmacol. Biomed. Anal.* **7**:699–707 (1989).
8. Nicholson, J. K., D. P. Higham, J. A. Timbrell, and P. J. Sadler. Quantitative high resolution NMR urinalysis studies on the biochemical effects of cadmium in the rat. *Mol. Pharmacol.* **36**:398–404 (1989).
9. Nicholson, J. K., and I. D. Wilson. High resolution proton NMR spectroscopy of biofluids. *Prog. NMR Spectrosc.* **21**:449–501 (1989).
10. Foxall, P., M. Bending, K. P. R. Gartland, and J. K. Nicholson. Acute renal failure following accidental cutaneous absorption of phenol: application of proton NMR urinalysis to monitor the disease process. *Hum. Toxicol.* **9**:491–496 (1989).
11. Evan, A. P., and W. G. Dail. The effects of sodium chromate on the proximal tubules of the rat kidney: fine structural damage and lysozymuria. *Lab. Invest.* **30**:704–715 (1974).
12. Haagsma, B. H., and A. W. Pound. Mercuric chloride-induced renal tubular necrosis in the rat. *Br. J. Exp. Pathol.* **60**:341–352 (1979).
13. Lock, E. A., and J. Ishmael. The acute effects of hexachlorobutadiene on the rat kidney. *Arch. Toxicol.* **43**:47–57 (1979).
14. Halman, J., and R. G. Price. Urinary enzymes and isoenzymes of *N*-acetyl-β-D-glucosaminidase in the assessment of nephrotoxicity, in *Selected Topics in Clinical Enzymology* (D. M. Goldberg and M. Werner, eds.), Vol. 2. Walter de Gruyter and Co., Berlin, 435–444 (1984).
15. Murray, G., G. Wyllie, G. S. Hill, P. W. Ramsden, and R. H. Heptinstall. Experimental papillary necrosis of the kidney. I. Morphologic and functional data. *Am. J. Pathol.* **67**:285–302 (1972).
16. Recknagel, R. O. Carbon tetrachloride hepatotoxicity. *Pharmacol. Rev.* **19**:145–208 (1967).
17. Gupta, D. N. Acute changes in liver after administration of thioacetamide. *J. Pathol. Bacteriol.* **72**:183–192 (1956).
18. Sanins, S. M. Nuclear magnetic resonance studies of xenobiotic metabolism and hepatotoxic processes in the rat. Ph.D. thesis, University of London (1988).
19. Capizzo, F., and R. J. Roberts. α-Naphthylisothiocyanate (ANIT)-induced hepatotoxicity and disposition in various species. *Toxicol. Appl. Pharmacol.* **19**:176–187 (1971).
20. Stein, J. H., J. Gottschall, R. W. Osgood, and T. F. Ferris. Pathophysiology of a nephrotoxic model of acute renal failure. *Kidney Int.* **8**:27–41 (1975).
21. Gartland, K. P. R., M. L. Anthony, C. R. Beddell, J. C. Lindon, and J. K. Nicholson. Proton NMR studies on the effects of uranyl nitrate on the biochemical composition of rat urine and plasma. *J. Pharm. Biomed. Anal.* **8**:951–954 (1990).
22. Reid, W. D. Mechanism of allyl alcohol-induced hepatic necrosis. *Experientia (Basel)* **28**:1058–1061 (1972).
23. Samarickmansinghe, G. P. Biological effects of cadmium in mammals, in *The Chemistry, Biochemistry and Biology of Cadmium* (M. Webb, ed.). Elsevier/North Holland Biomedical Press, Amsterdam (1979).
24. Bales, J. R., D. P. Higham, I. Howe, J. K. Nicholson, and P. J. Sadler. Use of high-resolution proton nuclear magnetic resonance spectroscopy for rapid multi-component analysis of urine. *Clin. Chem.* **30**:426–432 (1984).

25. RS1, Data Handling Softaware. BBN Software Products UK Ltd, Staines, Middlesex, UK (1988).
26. ARTHUR 81, Version 4.1. B & B Associates, Seattle, WA 98105 (1981).
27. Hansch, C., S. H. Unger, and A. B. Forsythe. Strategy in drug design: cluster analysis as an aid in the selection of substituents. *J. Med. Chem.* **16**:1217–1222 (1973).
28. Willett, P. *Similarity and Clustering in Chemical Information Systems*. Research Studies Press Ltd., Letchworth, UK (1987).
29. Jurs, P. C. Pattern recognition used to investigate multivariate data in analytical chemistry. *Science (Washington, D. C.)* **232**:1219–1224 (1986).
30. Kowalski, B. R., and C. F. Bender. Pattern recognition: a powerful approach to interpreting chemical data. *J. Am. Chem. Soc.* **94**:5632–5639 (1972).
31. Sammon, J. W. A non-linear mapping for data structure analysis. *IEEE Trans. Comput.* **C-18**:401–409 (1969).
32. Seal, H. *Multivariate Statistical Analysis for Biologists*. Methuen & Co. Ltd., London, 101–102 (1968).
33. Chatfield, C., and A. J. Collins. *Introduction to Multivariate Analysis*. Chapman and Hall, London, 57–59 (1980).
34. Hudson, B. D., D. J. Livingstone, and E. Rahr. Pattern recognition display methods for the analysis of computed molecular properties. *J. Comput. Aid. Mol. Des.* **3**:55–65 (1989).
35. Nash, J. A., L. J. King, E. A. Lock, and T. Green. The metabolism and disposition of hexachloro-1,3-butadiene in the rat and its relevance to nephrotoxicity. *Toxicol. Appl. Pharmacol.* **73**:124–137 (1984).
36. Anders, M. W., A. A. Elfarra, and L. H. Lash. Cellular effects of reactive intermediates: nephrotoxicity of *S*-conjugates of amino acids. *Arch. Toxicol.* **60**:103–108 (1987).
37. Elfarra, A. A., I. Jakobson, and M. W. Anders. Mechanism of *S*-(1,2-dichlorovinyl)glutathione-induced nephrotoxicity. *Biochem. Pharmacol.* **35**:283–288 (1986).
38. Newton, J. F., M. Yoshimoto, J. Berstein, G. F. Rush, and J. B. Hook. Acetaminophen nephrotoxicity in the rat. II. Strain differences in nephrotoxicity and metabolism of *p*-aminophenol, a metabolite of acetaminophen. *Toxicol. Appl. Pharmacol.* **69**:307–318 (1983).

Send reprint requests to: Dr. J. K. Nicholson, Department of Chemistry, Birkbeck College, University of London, Gordon House, 29 Gordon Square, London WC1H 0PP, UK.